

Integrated Supply-demand Energy Management for Optimal Design of Off-grid Hybrid Renewable Energy Systems for Residential Electrification in Arid Climates

**Charafeddine Mokhtara¹, Belkhir Negrou¹, Abdessalem Bouferrouk², Yufeng Yao²,
Noureddine Settou¹, Mohamad Ramadan³**

¹ Laboratoire de Promotion et Valorisation des Ressources Sahariennes (VPRS), Kasdi Merbah Ouargla University, BP 511, 30000 4 Ouargla, Algeria.

² Department of Engineering Design and Mathematics, University of the West of England, Bristol, BS16 1QY, UK.

³ Energy and Thermo-Fluid Group, School of Engineering, The International University of Beirut (BIU), Beirut, Lebanon.

The corresponding author of the manuscript:

Mr: Charafeddine Mokhtara

Tel.: +213 659 70 41 66

E-mail address: mokhtara.chocho@gmail.com; charaf92eddine@gmail.com; mokhtara.charafeddine@univ-ouargla.dz

Integrated Supply-demand Energy Management for Optimal Design of Off-grid Hybrid Renewable Energy Systems for Residential Electrification in Arid Climates

Charafeddine Mokhtara¹, Belkhir Negrou¹, Abdessalem Bouferrouk², Yufeng Yao²,
Noureddine Settou¹, Mohamad Ramadan³

¹ Laboratoire de Promotion et Valorisation des Ressources Sahariennes (VPRS), Kasdi Merbah Ouargla University, BP 511, 30000 4 Ouargla, Algeria.

² Department of Engineering Design and Mathematics, University of the West of England, Bristol, BS16 1QY, UK.

³ Energy and Thermo-Fluid Group, School of Engineering, The International University of Beirut (BIU), Beirut, Lebanon.

The corresponding author of the manuscript:

Mr: Charafeddine Mokhtara

Tel.: +213 659 70 41 66

E-mail address: mokhtara.chocho@gmail.com; charaf92eddine@gmail.com; mokhtara.charafeddine@univ-ouargla.dz

Abstract

The growing research interest in hybrid renewable energy systems (HRESs) has been regarded as a natural and yet critical response to address the challenge of rural electrification. Based on a Bibliometric analysis performed by the authors, it is concluded that most studies simply adopt supply-side management techniques to perform the design optimization of such a renewable energy system. To further advance those studies, this paper presents a novel approach by integrating demand-supply management (DSM) with particle swarm optimization and applying it to optimally design an off-grid hybrid PV-solar-diesel-battery system for the electrification of residential buildings in arid environments, using a typical dwelling in Adrar, South of Algeria, as a case study. The proposed HRES is first modelled by an in-house MATLAB code based on a multi-agent system concept and then optimized by minimizing the total net present cost (TNPC), subject to reliability level and renewable fraction (RF). After validation against the HOMER software, further techno-economic analyses including sensitivity studies are undertaken, considering different battery technologies. By integrating the proposed DSM, the results have shown the following improvements: with RF=100%, the energy demand and TNPC are reduced by 7% and 18%, respectively, compared to the case of using supply-side management only. It is found that PV-Li-ion represents the best configuration, with TNPC of \$23,427 and cost of energy (COE) of 0.23 \$/kWh. However, with lower RF values, the following reductions are achieved: energy consumption (19%) and fuel consumption or CO₂ emission (57%). In contrast, the RF is raised from 15% (without DSM) to 63% (with DSM). It is concluded that the optimal configuration consists of wind-diesel, with COE of 0.21 \$/kWh, smaller than that obtained with a stand-alone diesel generator system. The outcomes of this work provide valuable insights into the successful design and deployment of HRES in Algeria and surrounding regions.

Keywords: Hybrid renewable energy system; Energy management; Optimal design; Rural electrification; Building energy consumption; Multi agent-based particle swarm optimization.

Nomenclature

| | |
|-------------------|---|
| AC | Alternating Current |
| ACL | Agent Communication Language |
| BS | Battery Storage |
| CA | Control Agent |
| COE | Cost Of Energy |
| CRF | Capital Recovery Factor |
| DA | Design Agent |
| DC | Direct Current |
| DG | Diesel Generator |
| DSM | Demand-Supply Management |
| FIPA | Foundation of Intelligent Physical Agents |
| G | Solar Radiation (W/m^2) |
| GA | Generation Agent |
| HRES | Hybrid Renewable Energy System |
| HVAC | Heat Ventilation and Air Conditioner |
| JADE | Java Agent Development Framework |
| KT | Temperature Coefficient of Power |
| LA | Load Agent |
| LPSP | Loss of Power Supply Probability |
| MAS | Multi-Agent System |
| NASA | National Aeronautics and Space Administration |
| NBR | Number |
| NOCT | Nominal Operating Condition Temperature |
| PV | Photovoltaic |
| RER | Renewable Energy Resources |
| R _g | Ramping Factor |
| SA | Storage Agent |
| SOC | State of Charge of the Battery |
| STC | Standard (Reference) Test Conditions |
| t | Time Interval (One Hour) |
| T _c | Cell Temperature |
| T _{ref} | Reference Temperature |
| V _a | Actual Wind Speed |
| V _{ci} | Cut-In Wind Speed |
| V _{co} | Cut-Out Wind Speed |
| V _r | Rated Wind Speed |
| WT | Wind Turbine |
| P _{npv} | The rated power of a Pv system under Stc |
| P _{DG,R} | DG maximum power generation at (t) |
| P _{pv} | The output power of the Pv |
| G _{ref} | Solar radiation at Reference Conditions (E.G. 1000 W/M ²) |
| P _{pv} | Amount of power generation from solar PV at (t) |
| P _{dg} | Amount of power generation from DG at (t) |
| P _{wt} | Amount of power generation from WT at (t) |
| P _r | WT rated power |

1. Introduction

1.1. Background

Currently, buildings account for 40% of global electricity usage, making a share of up to 30% of total CO₂ emission [1]. Because of the development of new electric equipment and the intense use of smart devices, the demand for electricity has increased significantly in the Algerian building sector, with an annual increase rate of 8% since 2017 [2]. Although the majority of buildings in the country are grid-connected [3], there remain large numbers of small and rural communities that are unable to access the national electricity grid mainly due to the fact that they live at far away distances from towns and cities, especially those located in the Sahara region of the country. As connecting these areas with the national electricity grid is technically difficult, diesel generator (DG) is currently the only source used for rural electrification. Due to the steady increase in diesel fuel prices, the high cost for transportation, and concerns over its degradation and environmental effects, serving electricity to these remote areas using DG is becoming less attractive socioeconomically. Within this context, the Algerian Government has made great efforts towards developing and using renewable energy technologies in rural regions by installing a number of PV and wind power plants [4,5]. However, only a few megawatts have been installed in the Sahara region of the country until now. This is mainly due to the dependency of renewable energy technologies on the weather e.g. the effect of environmental factors (mainly dust wind) on the high cost of installation of PVs and other techno economic barriers. In order to solve these issues, hybrid renewable energy systems (HRESs) are becoming more popular and provide a reliable pathway to provide electricity for rural areas. Generally, an off-grid hybrid renewable energy system consists of at least one renewable source, one conventional source (mostly diesel generator) and/or an energy storage system (such as batteries). Recently, HRESs have attracted an increased interest from researchers and policymakers because of their technical and environmental benefits. The challenge in designing such a solution concerns its economic feasibility [6]. Clearly, this cannot be attained without the development of an energy management method, since an efficient management system will guarantee that HRES works in an efficient and economical way [7].

1.2. Literature review and current research gap

Much research work has been undertaken on the design of HRES, using various energy management and sizing approaches [8]. The optimal sizing of a hybrid wind/photovoltaic (PV) renewable energy system considering the effect of the wind turbine (WT) model was investigated by Mehrjerdi [9]. Abo-elyousr et al. [10] used a multi-objective optimization algorithm for the optimal design of HRES, considering a variety of alternative fuels. Tao and Javed [11] performed the sizing of a hybrid PV-wind-battery system for an island case study. Assaf [12] proposed an integrated solar-based HRES to supply remote areas with low cost renewable energy. The optimal design of PV-wind-battery HRES was also carried out by Tudu et al. [13]. The design optimisation of an off-grid hybrid renewable energy system including thermoelectric generators was discussed by Rodolfo et al. [14], in which minimising the net present cost was the main objective. Adefaratie and Bansal [15] evaluated the reliability, economic and environmental benefits of hybrid PV-wind-electric storage-diesel systems for rural communities. Jamshidi and Askarzadeh [16] optimized an off-grid HRES using multi-objective crow search algorithm (MOCSA). Moradi et al. [17] developed an energy management technique based on an advanced dynamic programming method for the best design of a stand-alone HRES. Eriksson [18] proposed a multi-objective approach by implementing a particle swarm optimization (PSO) for achieving a compromise between several techno-economic, environmental and socio-political objectives for the optimization of HRES. Zhang et al. [19] utilised an advanced heuristic technique to find an optimal configuration of a HRES, and later integrated a neural network (NN) weather forecasting system with an optimization algorithm for the optimal sizing of an off-grid HRES [20]. Both genetic algorithm (GA) and PSO algorithm were combined in the study by Mellouk et al. [21] to optimise a HRES. The economic evaluation of a micro-grid HRES was performed by Yu et al. [22]. Kaabeche and Bakelli [23] carried out the size optimization of a HRES considering various electrochemical energy storage technologies. Hamanah et al. [24] presented a new methodology to optimize a hybrid PV-wind-diesel-battery energy system, in which the minimization of the annual cost was the target objective function considering different constraints. Haratian et al. [25] used HOMER software to examine the techno-economic feasibility of a stand-alone HRES. Similarly, the sizing of a hybrid PV/diesel/battery energy system for a rural Saharan community in Algeria was investigated by Fodhil et al. [26], also using HOMER software. Fodhil [27] used PSO with the ϵ -constraint method for the optimal design of a PV/DG/battery hybrid energy system for rural

electrification in Algeria. Meanwhile, Duman et al. [28] conducted a technical and financial feasibility analysis for an off-grid hybrid system with variable climatic environments using HOMER software. Anoune [29] used a TRNSYS deterministic based approach to perform the sizing of a PV-wind based hybrid energy system for supplying electrical load demands in isolated areas. Jafar et al. [30] implemented a sizing method that integrated energy management to optimize the size of a stand-alone HRES using a flower pollination technique. Das et al. [31] carried out a techno-economic analysis and optimal design of an off-grid HRES using water cycle algorithm and moth-flame meta-heuristic optimization techniques for a radio transmitter station in India. Halabi et al. [32] carried out a performance analysis of a hybrid PV/diesel/battery system through HOMER software for a rural area case study in Malaysia. Rullo et al. [33] developed a bi-level optimization framework by integrating an energy management system to the GA based sizing method for optimal sizing of a hybrid PV/wind energy system with energy storage.

Although the optimal sizing of HRES is always an important task, peak load shaving is becoming ever more necessary for limiting the rapid growth in residential energy demand [34]. Peak-load shaving can also help to address the oversizing problem in HRES, and in the meantime to reduce the system cost. Generally, peak load shaving is defined as a way to flatten the load by either limiting the peak load or shifting some loads to lower demand periods [35]. From the literature, three peak-load shaving strategies are identified: 1) the integration of an energy storage system, 2) vehicle to home (V2H) technology, and 3) demand-side management or demand response. Tu et al. [36] carried out a multi-layered demand scheduling using Mixed Integer Linear Programming for the optimization of hybrid PV/wind/DG/battery system with the aim of minimizing the cost of energy (COE). In a study carried out by Rullo et al. [37], the optimization of a biomass-based microgrid with demand-supply management (DSM) was performed to minimize the operating cost of a biomass combined heat and power microgrid, using a load shifting algorithm based on economic linear programming of a model predictive control. Similarly, Yang et al. [38] carried out a techno-economic and environmental optimization of a PV/battery hybrid energy system within DSM. Sarkar et al. [39] undertook an optimal design of a hybrid solar PV/wind/biogas/battery energy system for ensuring higher system reliability through the use of HOMER software. In their work, a demand-side management (i.e. peak load shaving) strategy was established. Wu et al. [40] presented a demand-side management technique for optimal operation of a hybrid PV/battery energy system. Thiaux et al. suggested a DSM strategy to find out the best configuration of a HRES for off-grid regions. [6]. Mohseni et al. proposed a novel method incorporating a demand response technique for the optimal sizing of an off-grid hybrid PV/wind turbine/battery/electric vehicle, subject to satisfying a reliability index for meeting the required loads [41].

From these aforementioned literature and based on an extensive Bibliometric analysis of some 699 published papers on the topic over the last ten years (from the Elsevier database), and using the first four keywords of this study, as shown in Fig. 1 (using VOS viewer tool), the following observations can be made:

- 1) The majority of works on the optimization of HRESs have been focused on techno-economic parameters such as the net present cost and system reliability;
- 2) The particle swarm optimization and HOMER software are the most used optimization techniques;
- 3) The solar, wind energy and battery are the most used renewable source and storage system, respectively;
- 4) Most of the studies are focused on supply-side management to ensure the demands are met even during the peak periods. In contrary, little work has been done for the effect of peak load shaving on the optimal design of HRES.

Besides, those applied demand-side management techniques such as load shifting were merely feasibility studies for the non-primary load (such as washing machine and water pumping). Therefore, there have been no demand-side management strategies implemented until now for primary loads (such as air conditioning and other HVAC systems) in the optimisation of HRES. This can be demonstrated by the recommendations of a review paper conducted recently [35], in which the authors suggested that future works should be focused on the proper application of demand-side management and the transition towards smart home technologies. Thus, an integrated management system that enables controlling both sides (i.e. supply-side and demand-side) could provide a broader range of opportunities in optimizing the overall energy management system [37] and to ensure the optimal design and operation of HRES.

2. System modelling and configuration

In this work, a new approach is proposed for the energy management and the size optimization of a HRES to provide the electricity needs for an off-grid residential building in Adrar, south of Algeria. The studied hybrid system is shown in Fig. 2, including PV solar panels, small wind turbines (WT), DG, battery storage, and a power converter.

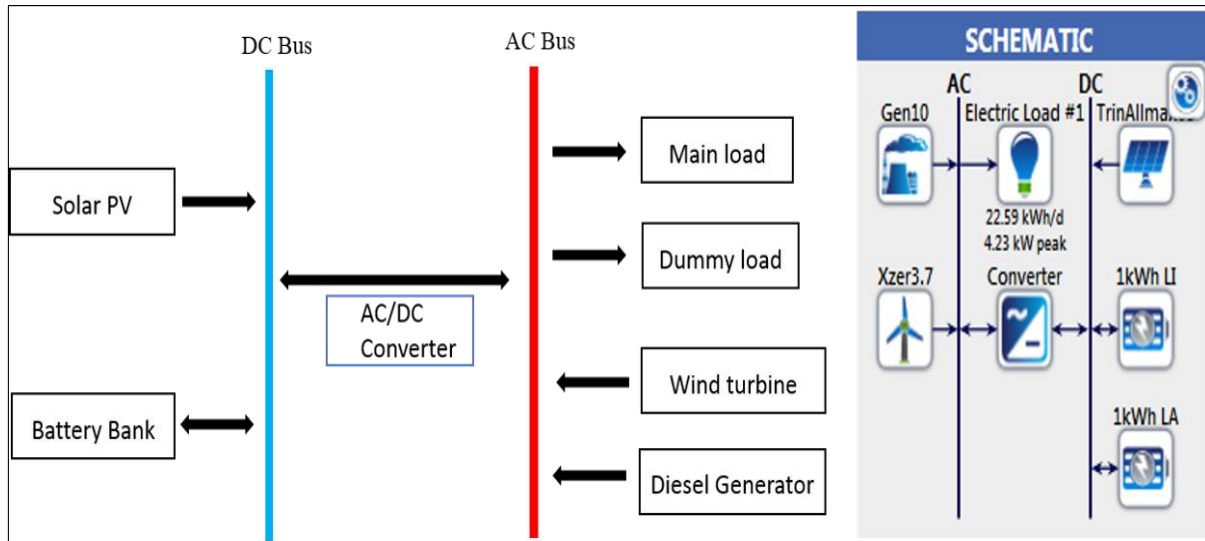


Figure 2. Schematic view of the investigated hybrid renewable energy system.

Decentralized controlling systems such as multi-agent systems (MAS) are more and more prominent with the growing demands in distributed energy systems. There are many tools for the implementation of MAS, including JADE. JADE framework is an open-source agent-oriented middleware with the most widespread use of this kind. Agents in MAS are autonomous and can use messages to interact and understand the environment. Communication among agents in JADE is implemented based on FIPA-specified agent communication language (FIPA-ACL), which is the most important standardization activity conducted in the field of agent technology. JADE can be integrated with MATLAB software platform. The MAS-based framework for the simulation of the suggested HRES in MATLAB has been introduced in this work, in which five agents are defined:

1. **Load Agent (LA):** This agent is responsible for calculating and controlling hourly loads, and provides the required information to other agents. It also receives climatic data from the environment.
2. **Generation Agent (GA):** All energy sources including WT, solar PV, and diesel generator are included in the generation agent. This agent is in charge of evaluating the state of the sources of supply and provides information every hour on the available energy potential. It is responsible for adding, deleting, changing, connecting or disconnecting any energy source.
3. **Storage Agent (SA):** SA includes a battery bank. The SA has permanent behaviour, because it can work in case of charge and/or discharge. However, this agent has some charge limits, i.e. at each hour the SA supervises the state of charge of batteries and receives information from GA and LA to decide when batteries could run on charge or discharge mode.
4. **Design Agent (DA):** DA is an independent system operator responsible for the optimization of the HRES. This agent selects and refines the size of the HRES' components to find out the optimal configuration of HRES.
5. **Control Agent (CA):** CA is the supervisor of the system and is solely concerned with the monitoring of the different information according to expectations from/to other agents.

The following sub-sections describe the mathematical models of the five agents above and the information flow chart between them.

2.1. Load agent

2.1.1. Building description

As this study is concerned with the effective design of HRES to satisfy the electricity needs of households in remote parts of Algeria, for that reason, a typical residential building is selected as a case study, which is known as 'F2' according to Algerian standards of construction [42]. The building includes a bedroom, a sitting room, a corridor, a kitchen, and a bathroom. The whole floor area is 64 m². The height of the building is 3 m. In Fig. 3, both 2D floor plan view and 3D building model (using a design builder software) are presented. In addition, the characteristics of the building are provided in Table 1.

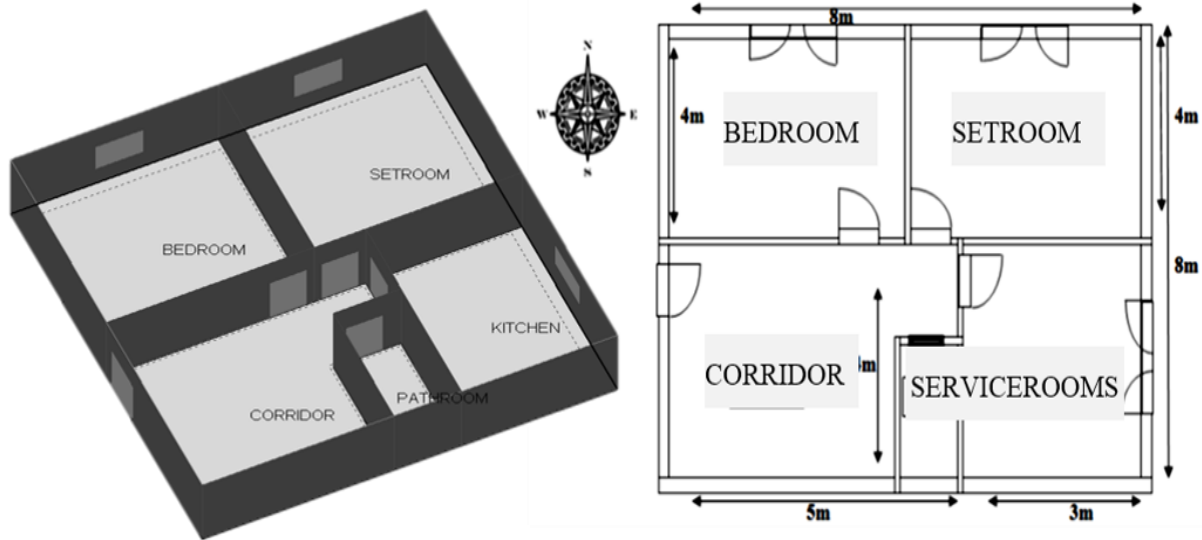


Figure 3. The layout of the building.

Table 1. Building components and characteristics of walls.

| Element | Construction (outside to inside) (m) | U-value (W/m ² K) |
|---------------|---|------------------------------|
| Ground floor | Concrete (0.1), Extruded Polystyrene (0.04), Concrete (0.1), Ceramic floor tiles (0.02) | 0.573 |
| Roof | Bitumen (0.01), Cement (0.01), Concrete Block (0.2), Cement (0.01) | 2.994 |
| Internal Wall | Cement (0.01), Brick (0.1), Cement (0.01) | 2.079 |
| External Wall | Cement (0.01), Brick (0.1), Air gap (0.01), Brick (0.1), Cement (0.01) | 1.39 |
| Glazing | / | 1.978 |
| Door | / | 2.823 |

2.1.2. Geographic location and climatic data

The building is simulated under the climate of Adrar, Sahara of Algeria, where the temperature and relative humidity can reach 50°C and 5 % in summer. The hourly climatic data for Adrar, over an entire year (as an average of 10 years, from 1990 to 2010), are extracted from Meteonorm software. The hourly ambient temperature and wind speed in Adrar are presented in Fig. 4 and Fig. 5, respectively. In addition, the daily average solar irradiation (G) and clearness index (CI) at each month of the year are given in Fig. 6.

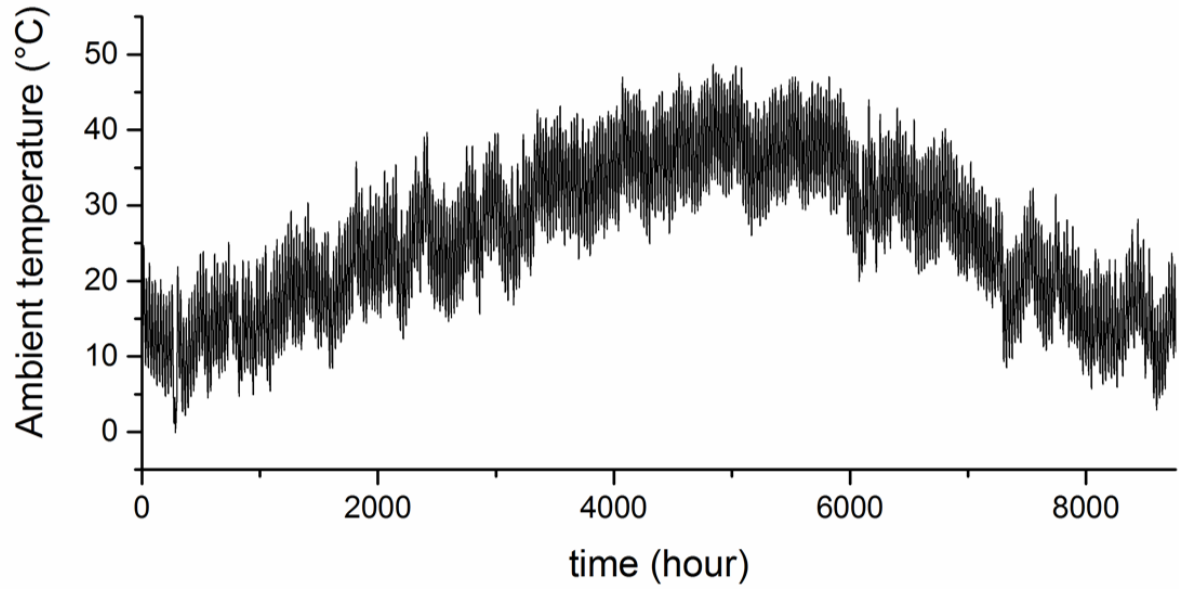


Figure 4. The hourly ambient temperature at Adrar region, Algeria.

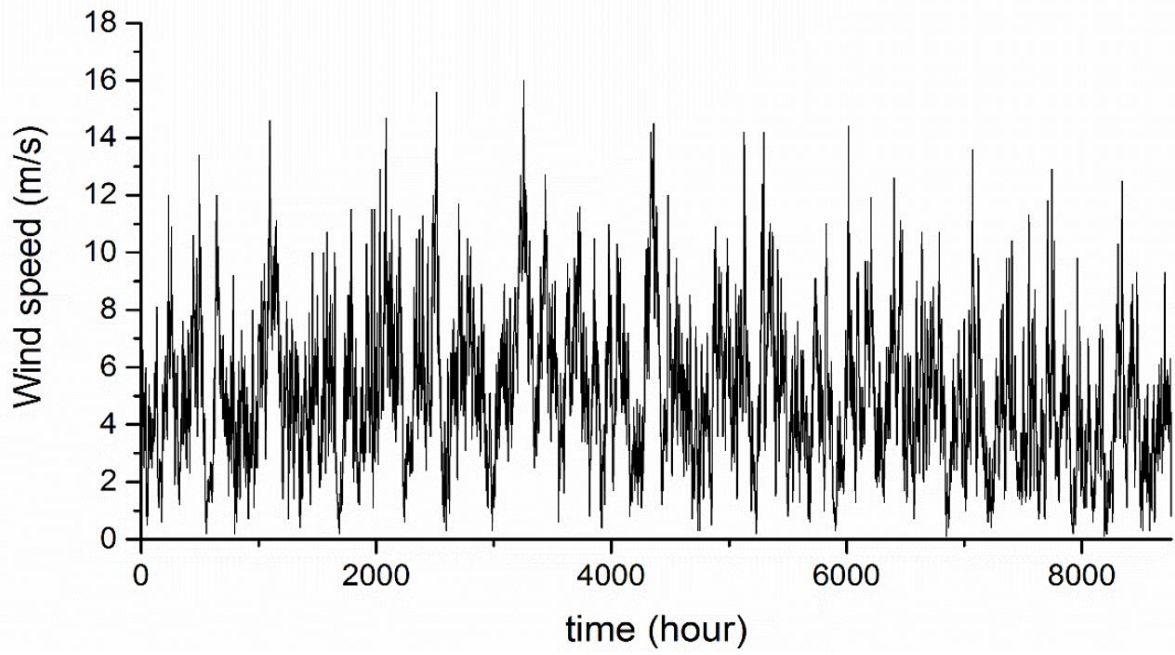


Figure 5. Hourly wind speed at Adrar region, Algeria.

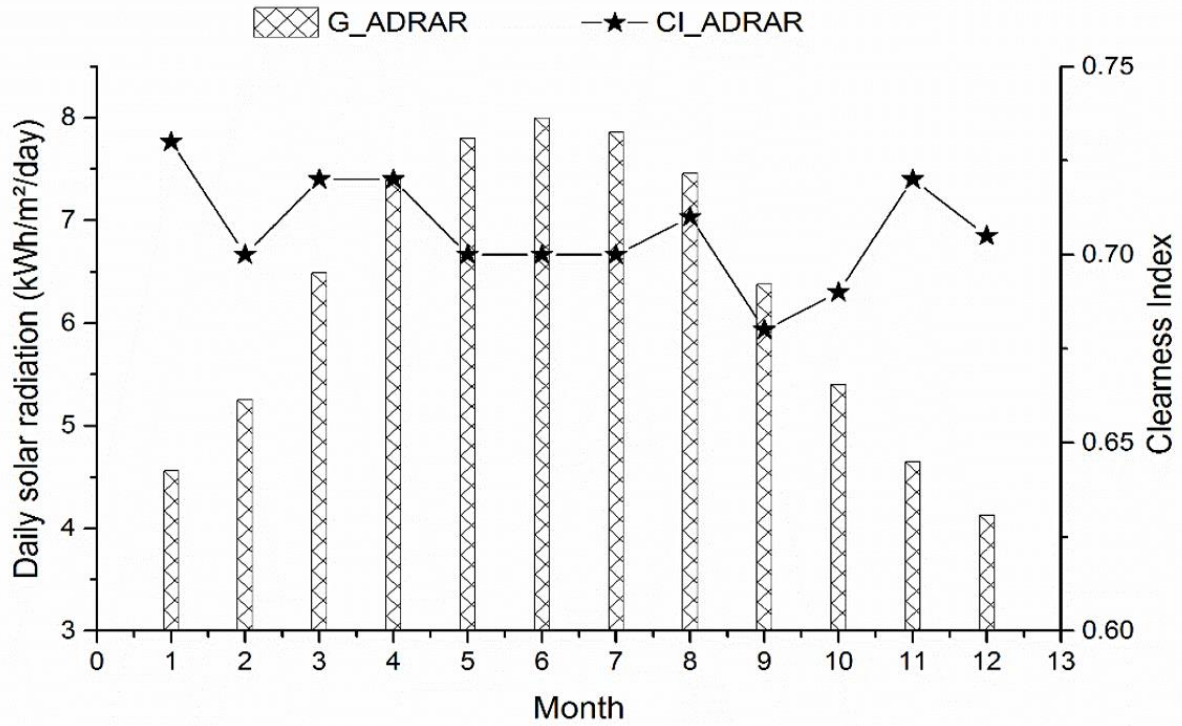


Figure 6. Daily average solar radiation and clearness index in Adrar, Algeria.

2.1.3. Load estimation

The load profile of the studied building is divided into two parts. The first part includes all different electric devices, except for the cooling chiller. Hence, the second part includes the load profile of space cooling which is evaluated by Energy Plus software [43].

The primary concern is the hourly electricity demand for the building's appliances, which includes a refrigerator, a lighting system, and a TV. This load is evaluated based on the number and the rated power of each device, and the usage time of occupants. Table 2 gives a summary of the building appliances and their characteristics. The hourly demand for electric appliances per day on average over the year is provided in Fig. 7.

Table 2. Building appliances and their characteristics.

| Element | Rated power (W) | Number | Daily use (hours) |
|--------------|-----------------|--------|-------------------|
| Refrigerator | 320 | 1 | 24 |
| Light | 40 | 5 | 18 |
| TV | 100 | 1 | 8 |

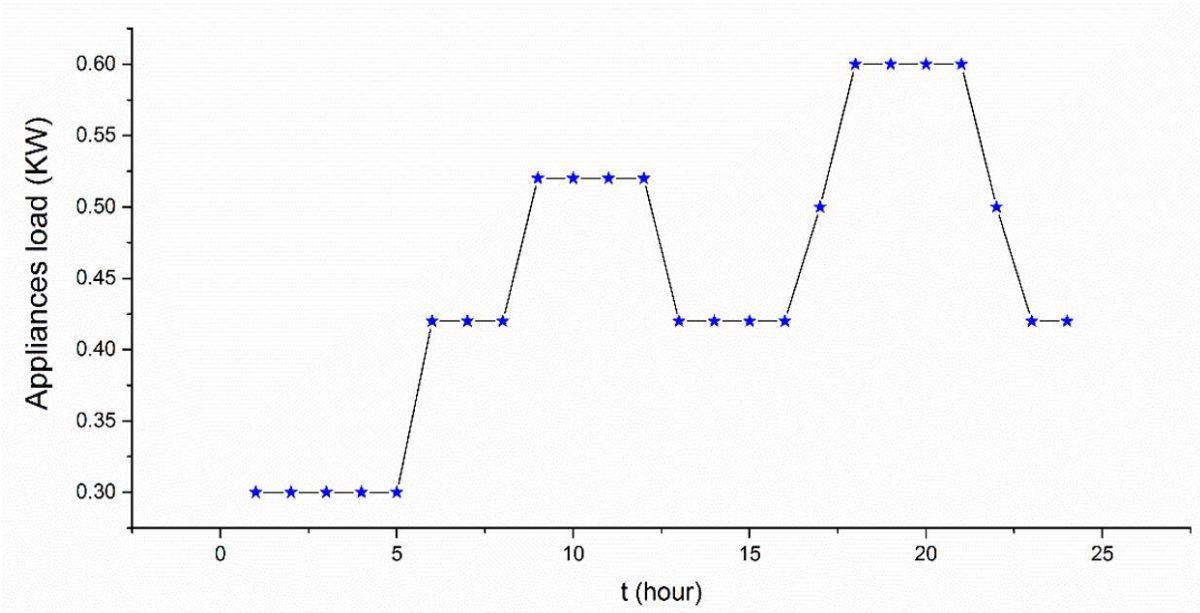


Figure 7. Profile of electricity demand for appliances per day.

The secondary load includes the demand for heating, ventilation, and air-conditioning (HVAC) systems which are the major energy consumption devices in the building and thus become ideal candidates for substantial reductions in energy demand [1]. In hot dry climates as in Adrar, the required demand for space cooling is assumed more than half of the total electricity demand. To evaluate the energy demand for space cooling of the investigated building, here both Energy Plus and Design Builder software are used. Only the bedroom and the sitting room have an air conditioner each. Thus, the conditioned floor area is 32 m². Fig. 8 shows the hourly demand for space cooling in case of 24°C (that corresponds the desired temperature for high level of thermal comfort) and 29°C set point temperature (a suggested desired temperature for cooling for very hot locations, where the outside temperature can exceed 60 °C).

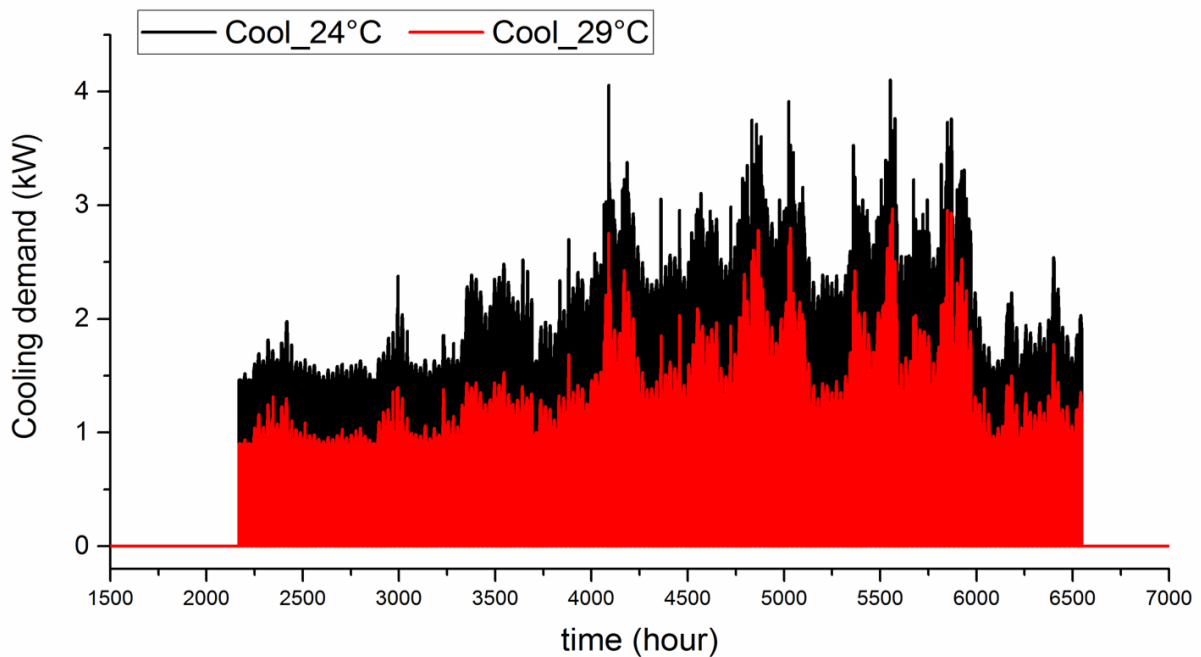


Figure 8. Energy demand for space cooling during summer period.

The global electricity demand of the building including both loads is then assumed for both desired temperatures in cooling mode. With a 24 °C set point temperature, the global demand is found to be 8698

kWh/year. However, for a desired set point temperature of 29 °C, the overall demand of the building is found to be 6948 kWh/year.

2.2. Generation agent

Generation agent includes all produced sources, including renewable and non-renewable sources. The mathematical modelling of this agent and their components are provided as follows.

2.2.1. Solar PV

Solar PV panel is a device that converts solar energy into electric energy. The energy delivered by the PV could be quantified based on the solar radiation and the air temperature as given in Eq. 1 [44]:

$$P_{pv} = P_{Npv} \times \frac{G}{G_{ref}} \times \left[1 + K_t \times \left(\left[T_{amb} + \frac{NOCT - 20}{800} \right] \times G - T_{ref} \right) \right] \quad (1)$$

where P_{pv} is the rated power of the PV system. G and G_{ref} represent solar radiation at time t and at standard conditions, respectively. T_{amb} and T_{ref} are the ambient temperature at time t and at standard conditions respectively. K_t is the temperature coefficient of power and its value depends on the PV panel's technology.

2.2.2. Wind Turbine (WT)

The wind turbine is used to produce electricity from the kinetic energy available in the wind flow. The power output of the WT P_{wt} can be computed using Eqs. 2-4, as follows [45]:

$$P_{wt} = 0 \quad \text{if } V < V_{cut_{in}} \text{ or } V > V_{cut_{out}} \quad (2)$$

$$P_{wt} = V^3 \left(\frac{Pr}{Vr^3 - V_{cut_{in}}^3} \right) - \left(\frac{V_{cut_{in}}^3}{Vr^3 - V_{cut_{in}}^3} \right) \times Pr \quad \text{if } V > V_{cut_{in}} \text{ and } V < Vr \quad (3)$$

$$P_{wt} = Pr \quad \text{if } V > Vr \text{ and } V < V_{cut_{out}} \quad (4)$$

where Pr is the rated power of the WT. V is the wind speed at the studied location (for each hour). The $V_{cut_{in}}$, $V_{cut_{out}}$, V_r represent cut in, cut out and rated wind speed of WT respectively (normally provided by the manufacturer).

2.2.3. Diesel generator (DG)

DG is used in a hybrid energy system to meet the load demand in case the total available power generated from renewable energy and batteries is not sufficient. The amount of consumed fuel by DG is dependent on its output power at each time step as expressed by Eq. 5 [46]:

$$F_{cons} = a \cdot P_{DG} + b \cdot P_{DG,r} \quad (5)$$

where $P_{DG}(t)$ is power generated by DG (kW) at each hour (t), F_{cons} is fuel consumption (L/h), $P_{DG,r}$ is the rated power of DG generated at each hour (t), a and b are constants (L/kW), which represent the coefficients of fuel consumption, with standard values of 0.08415 and 0.246, respectively.

2.2.4. Converter

The power converter is a device that converts the electrical energy from AC into DC or vice versa. The rated power of a converter depends on the peak load. The efficiency of the converter is evaluated by Eq. 6 [27].

$$\eta_{cnv} = \frac{P_{output}}{P_{input}} \quad (6)$$

where P_{output} and P_{input} are the output and the input power from/to converter, respectively.

2.3. Storage agent

In this study, the storage agent solely includes batteries, which are easy to install and possess high energy efficiency. Excess electricity from renewable sources is used to start charging the battery, while it can be used in the event of energy shortages. The state of charge of a battery in the discharge and the charge settings could be determined by Eqs. 7-8, respectively [46].

$$E_b(t+1) = E_b(t) \times (1 - \sigma) - \left(\frac{E_l(t)}{\eta_{cnv}} - E_g(t) \right) \times \eta_{BD} \quad (7)$$

$$E_b(t+1) = E_b(t) \times (1 - \sigma) + \left(E_g(t) - \frac{E_l(t)}{\eta_{cnv}} \right) \times \eta_{BC} \quad (8)$$

where $E_l(t)$ and $E_g(t)$ are the energy demand and generated power, respectively. η_{BD} and η_{BC} represent the discharge and charge efficiencies of the battery. Parameter σ is the self-discharge of the battery, which is set to be

zero in this study. η_{cnv} is efficiency of the converter. At each time step t , the state of charge of a battery $E_b(t)$ is constrained by the minimum and the maximum capacities of the storage E_{bmin} and E_{bmax} as specified in Eq. 9:

$$E_{bmin} \leq E_b(t) \leq E_{bmax} \quad \text{Where } E_{bmin} = (1 - DOD) \times E_{bmax} \quad (9)$$

where DOD is the depth of discharge of the battery, which depends on the battery's technology.

As batteries are not 'clean' energy storage systems, having a high cost of investment and a short life span [47], it is thus mandatory to select the best battery technology to reduce their capacity as much as possible. In this context, two battery technologies are considered, namely Lead-acid and Li-ion, both having different technical-economic characteristics.

2.4. Design agent (DA)

DA is the agent that performs the optimization of the HRES. In this study, DA is incorporated into the PSO algorithm, which works well to minimize the objective function and thus obtain the best HRES size. The objective function to be minimized is the cost of energy of the HRES, concerning the critical value of loss of power supply probability (LPSP). The critical value of LPSP is set at 1%, which represents the allowable loss of power for the entire yearly demand. Further, fuel consumption can be minimized to achieve the increased share of renewable energy.

2.5. Problem formulation

In this study, total net present cost (TNPC) is another objective function to be minimised as defined by the objective function (f) in Eq. 10, in which five decision variables (i.e. capacity of PV panels, batteries, diesel generator, converter and number of wind turbines) must be optimally sized, subject to constraints defined in Eqs. 11-13:

$$f = \min \cdot TNPC(P_{PV,r}, N_{WT,r}, P_{DG,r}, E_{bmax}, P_{Cnv,r}) \quad (10)$$

$$0 \leq LPSP \leq LPSP^{max} \quad (11)$$

$$RF^{min} \leq RF \leq 1 \quad (12)$$

$$0 \leq P_{PV,r}, N_{WT,r}, P_{DG,r}, E_{bmax}, P_{Cnv,r} \leq P_{PV,r}^{max}, N_{WT}^{max}, P_{DG,r}^{max}, BS^{max}, P_{Cnv}^{max} \quad (13)$$

More details of the mathematical formulae of the objective function, constraints and techno-economic and environment evaluating criteria are provided in the following subsections.

2.5.1. Total Net Present Cost (TNPC)

TNPC is widely used in the design of HRES. It can be evaluated based on Eqs. 11-18 [48].

$$TNPC(\$) = (C_{cap} + C_{O\&M} + C_{rep} + C_{fuel}) \quad (14)$$

where C_{cap} , C_{rep} , $C_{O\&M}$, C_{fuel} are the costs of investment, replacement, operation and maintenance and the cost of fuel, respectively.

$$C_{cap}(\$) = (P_{PV,r} \cdot C_{PV} + P_{WT,r} \cdot C_{WT} + P_{DG,r} \cdot C_{DG} + E_{bmax} \cdot C_{BS} + P_{Cnv,r} \cdot C_{Cnv}) \quad (15)$$

$$C_{O\&M}(\$) = 0.02 \cdot C_{Acap} \cdot \sum_{k=1}^T \frac{1}{(1+i)^k} \quad (16)$$

$$C_{rep}(\$) = \left(E_{bmax} \cdot C_{BS} \cdot \sum_{k=10}^T \frac{1}{(1+i)^k} + P_{Cnv} \cdot C_{Cnv} \cdot \sum_{k=12}^T \frac{1}{(1+i)^k} + P_{DG,r} \cdot C_{DG} \cdot \sum_{k=a,2a,\dots,<T}^T \frac{1}{(1+i)^k} \right) \quad (17)$$

$$C_{fuel}(\$) = fuel_{cons} \cdot C_{fuel} \cdot \sum_{k=1}^T \frac{1}{(1+i)^k} \quad (18)$$

where P_{Npv} , $P_{WT,r}$, $P_{DG,r}$, P_{Cnv} , E_{bmax} represent the rated power and the capacity of PV, WT, DG, converter, and battery, respectively. C_{PV} , C_{WT} , C_{DG} , C_{Cnv} , C_{BS} represent the investment and replacement costs of PV, WT, DG, converter, and battery, respectively. Here, $fuel_{cons}$ is fuel consumption.

2.5.2. Loss of power supply probability (LPSP)

LPSP is widely used to evaluate the system reliability. Generally, LPSP is the ratio of the total energy deficit over the total energy demand during one year of operation. LPSP represents the rate of dissatisfaction of the load and its value can be determined by Eq. 19 [11]:

$$LPSP(\%) = \frac{\sum_{t=1}^T E_l(t) - P_{PV}(t) - P_{WT}(t) - P_{DG}(t) - (Eb(t) - Eb_{min})}{\sum_{t=1}^T P_{load}(t)} \quad (19)$$

2.5.3. Renewable fraction (RF)

RF is introduced to set the minimum value of renewable energy contribution in the overall load served by the HRES. RF can be evaluated using Eq. 20 [49].

$$RF(\%) = 1 - \frac{\sum P_{DG}}{\sum P_{PV} + P_{WT} + P_{DG}} \quad (20)$$

2.5.4. Cost of energy (COE)

COE is obtained by dividing the total cost of the system (including costs related to the initial investment and all costs associated with the operation of the system components) by the annual energy served as given by Eq. 21.

$$COE(\$/kWh) = \frac{C_{Annualized}}{E_{served}} \quad (21)$$

where $C_{Annualized}$ and CRF are the total annualized cost and capital recovery factor, respectively, which are defined by Eqs. 22-23 as follows.

$$C_{Annualized}(\$) = TNPC \cdot CRF \quad (22)$$

$$CRF = \frac{[i(i+1)^T]}{[(i+1)^T - 1]} \quad (23)$$

where T is the project lifetime, and i is the real interest rate.

2.5.5. Fuel consumption and CO₂ emission

As most remote areas suffer from the high cost of fuel associated with its transport, it is also important to reduce fuel consumption. Besides, CO₂ emissions are also evaluated based on the amount of consumed fuel. Eqs. 24-25 are used to evaluate the consumed fuel and generated CO₂ by the HRES [50].

$$Fuel\ consumption(L/year) = \sum_{t=1}^{8760} fuel_{cons}(t), \quad (24)$$

$$CO_2(kg/year) = EF \cdot Fuel\ consumption \quad (25)$$

where EF is the emission factor of the DG, which depends on the type of diesel engine fuel properties. The value of this factor is in a range of 2.4 - 2.8 kg/lit [50]. This study takes a lower value of 2.4 kg/lit.

2.6. Particle swarm optimization (PSO) algorithm

PSO is considered to be the most frequently used method in the field of artificial intelligence [51]. This meta-heuristic optimization technique was firstly introduced by Kennedy and Eberhart in 1995 [27]. In PSO, a set of particles (also known as swarm), defined by their positions and velocity vectors, move through the search space seeking to reach their local optimum and global optimum for the swarm. Therefore, there are two optimum values to determine each particle's position. The first is the optimum value that has been achieved by each particle (i.e. local maximum) and the second is the optimum value obtained for the entire population (i.e. global maximum). The ultimate goal is to achieve the optimal solution for the objective function. The PSO algorithm solves the defined problem according to the following steps:

2.6.1. Step 1: Initialization

- (1) Load the hourly solar irradiation, ambient temperature, wind speed and building load for an entire year.
- (2) Load the components characteristics and economic parameters as presented in Table 3.
- (3) Set the constraints limits for LPSP and RF, and set the decision variables limits (including the minimum and the maximum values for each variable) as given by Table 4, and set a random value for them.

Table 3. HRES' components and economic parameters.

| Generation source | Parameters | Specification |
|-------------------|--------------------|---------------|
| Solar PV | Nominal power (kW) | 1 |

| | | |
|----------------------------|---|-----------|
| | Capital cost (\$/kW) | 1600 |
| | O&M cost (% of Capital cost) | 2 |
| | Temperature coefficient of power (%/°C) | -0.41 |
| | Lifetime (Year) | 20 |
| Wind turbine | Nominal power (kW) | 2.1 |
| | Capital cost (\$/kW) | 3000 [52] |
| | O&M cost (% of Capital cost) | 2% |
| | Cut-in speed (m/s) | 3 |
| | Cut-out speed (m/s) | 20 |
| | Rated speed (m/s) | 11 |
| | Lifetime (Year) | 20 |
| Diesel generator | Rated power (kW) | 1 |
| | Capital cost (\$/kW) | 800 [36] |
| | O&M cost (% of Capital cost) | 2% |
| | Fuel price (\$/L) | 0.2 |
| | Lifetime (hour) | 30000 |
| Lead-acid (L-acid) Battery | Battery capacity (kWh) | 1 |
| | Capital cost (\$/kWh) | 180 |
| | O&M cost (% of Capital cost) | 2 |
| | DOD (%) | 60 |
| | Discharge efficiency | 90% |
| | Charge efficiency | 100% |
| | Lifetime (Year) | 5 |
| Lithium-ion Battery | (Li-ion) Battery capacity (kWh) | 1 |
| | Capital cost (\$/kWh) | 300 |
| | O&M cost (% of Capital cost) | 2 |
| | DOD (%) | 80 |
| | Discharge efficiency | 90% |
| | Charge efficiency | 100% |
| | Lifetime (Year) | 10 |
| Converter | Capital cost (\$/kW) | 700 [52] |
| | O&M cost (% of Capital cost) | 2 |
| | Efficiency (%) | 95 |
| | Lifetime (Year) | 10 |
| Economic parameters | Project lifetime (Year) | 20 |
| | i (interest rate) (%) | 5 |

Table 4. Decision variables and constraints limits.

| Parameters | P_{PV} [kW] | N_{WT} [Nbr] | BS [kWh] | P_{DG} [kW] | Converter [kW] | LPSP [%] | RF [%] |
|------------|------------------|-------------------|-------------|------------------|-------------------|-------------|-----------|
| Min bound | 0 | 0 | 0 | 1 | 0 | 0 | 0 |
| Max bound | 9 | 2 | 40 | 5 | 10 | 2 | 100 |

2.6.2. Step 2: Initialization of PSO parameters

To determine ω , C_1 , and C_2 , the following coefficients must be calculated using Eqs. 26-27 [18]:

$$\varphi = \frac{2K}{2 - \varphi - \sqrt{\varphi^2 - 4\varphi}} \quad (26)$$

$$\varphi = \varphi_1 + \varphi_2 \geq 4 \quad (27)$$

where φ is the constriction coefficient. Typically, ϕ_1 and ϕ_2 are set to 2.05. The constant k is generally less than unity. Hence, ω , C_1 , and C_2 are calculated using Eqs. 28-30:

$$\omega = \varphi \quad (28)$$

$$C_1 = \varphi \cdot \phi_1 \quad (29)$$

$$C_2 = \varphi \cdot \phi_2 \quad (30)$$

Further settings of the PSO and simulation parameters are given in Table 5 [53].

Table 5. Parameters of the PSO.

| Parameter | Value |
|---------------------------------------|-------|
| Number of iterations | 100 |
| Population Size | 25 |
| The dimension of the search variables | 5 |
| k | 0.75 |
| constriction coefficients (both) | 2.05 |

2.6.3. Step 3: Determine particles' positions and fitness

- (1) Initialization of particle' velocity and position for all the population,
- (2) Evaluation of the fitness of each particle, and evaluate the optimal value for the initial population (i.e. the minimum TNPC)

2.6.4. Step 4: Estimate the new positions

- (1) Updating the optimum individual and global fitness and locations, and
- (2) Updating the velocity and location of each particle.

The location and the velocity of each particle in the swarm can be adjusted using Eqs. 31-32 [50]:

$$X_{k+1}^i = X_k^i + v_{k+1}^i \quad (31)$$

where X is particle position and v is particle velocity in iteration k :

$$v_{k+1}^i = [\omega v_k^i + C_1 r_1 (P_k^i - X_k^i) + C_2 r_2 (P_k^g - X_k^i)] \quad (32)$$

where V_k^i is named the inertia, which drives the particle to move at an indicated velocity towards a position. The term $C_1 r_1 (P_k^i - X_k^i)$ is the learning parameter. $C_2 r_2 (P_k^g - X_k^i)$ is so-called the social component, P_i is the optimal individual particle position and P_g is the optimal global position, C_1 and C_2 are personal (cognitive) and global (social) learning coefficients, respectively; r_1 and r_2 are random numbers (their values are between 0 and 1), ω is a coefficient.

The procedure is reproduced until all pre-defined conditions have been met, such as the number of iterations or pre-defined goal fitness levels.

2.6.5. Step 5: Output of obtained results

After the simulation is finished, key results are either plotted or exported in tabular forms for presentation and further analysis shown later.

2.7. Control Agent (CA)

CA is in charge of monitoring the components of the HRES. This agent follows an energy management strategy to ensure a balance between the demand and the supply sides and to ensure a compromise between the objective functions (cost, reliability, etc.) and to find the optimum size of HRES. As stated earlier, a DSM approach has been built and integrated into the optimization model. The DSM plan was proposed to reduce the energy usage of buildings and thus to avoid the oversizing of the HRES. Two loads are introduced in the optimization, the first is evaluated with a set point temperature in cooling mode at 24°C; and the second is evaluated at a set point temperature of 29°C. Hence, the main steps of the size optimization of the suggested HRES are as follows:

Case 1: Renewable sources (both solar and wind) supply sufficient electricity and any excess electricity will be used to charge the battery.

Case 2: Same as Case 1 except that the unused generated energy (as it is greater than the need for building consumption while the battery is fully charged) is transferred to the dump load.

Case 3: Renewable resources fail to provide sufficient energy to meet the first load (at 24°C). Therefore, the control agent requests to use the second load (at 29°C). If the system is still unable to provide the required load, then in this scenario the priority is to use the stored energy in the batteries rather than operating the diesel generator. Thus, DG still remains as the last option.

Case 4: The electricity provided from renewable sources is not sufficient to meet the required load and the battery bank is drained. In this case, DG is turned on to deliver the power. When the overall system fails to meet the demand, the loss of power supply is therefore evaluated.

The sequence diagram that illustrates the different interactions between the five agents, is presented in Fig. 9. Besides, a flowchart of the proposed optimization model including the developed DSM is presented in Fig. 10.

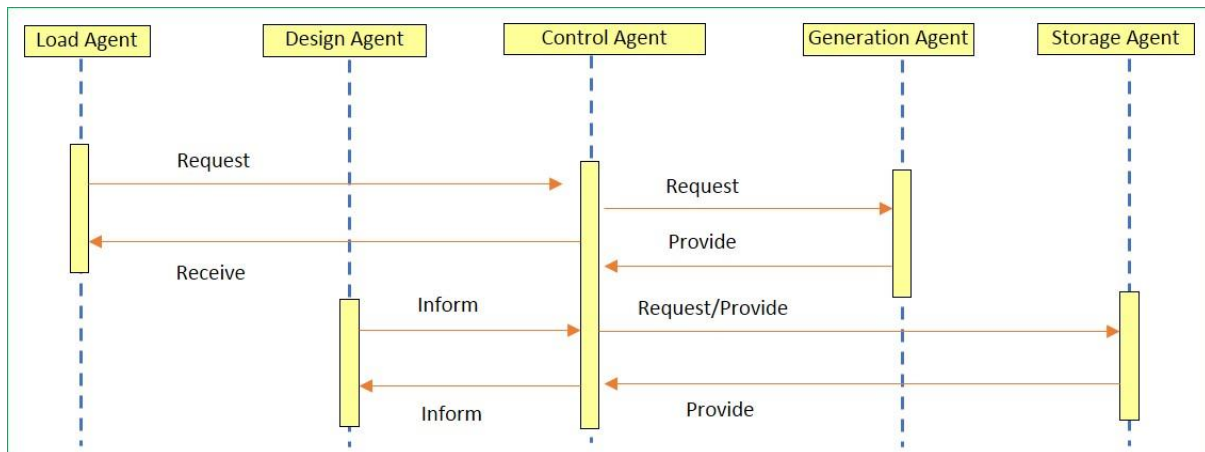


Figure 9. The sequence diagram of MAS for HRES

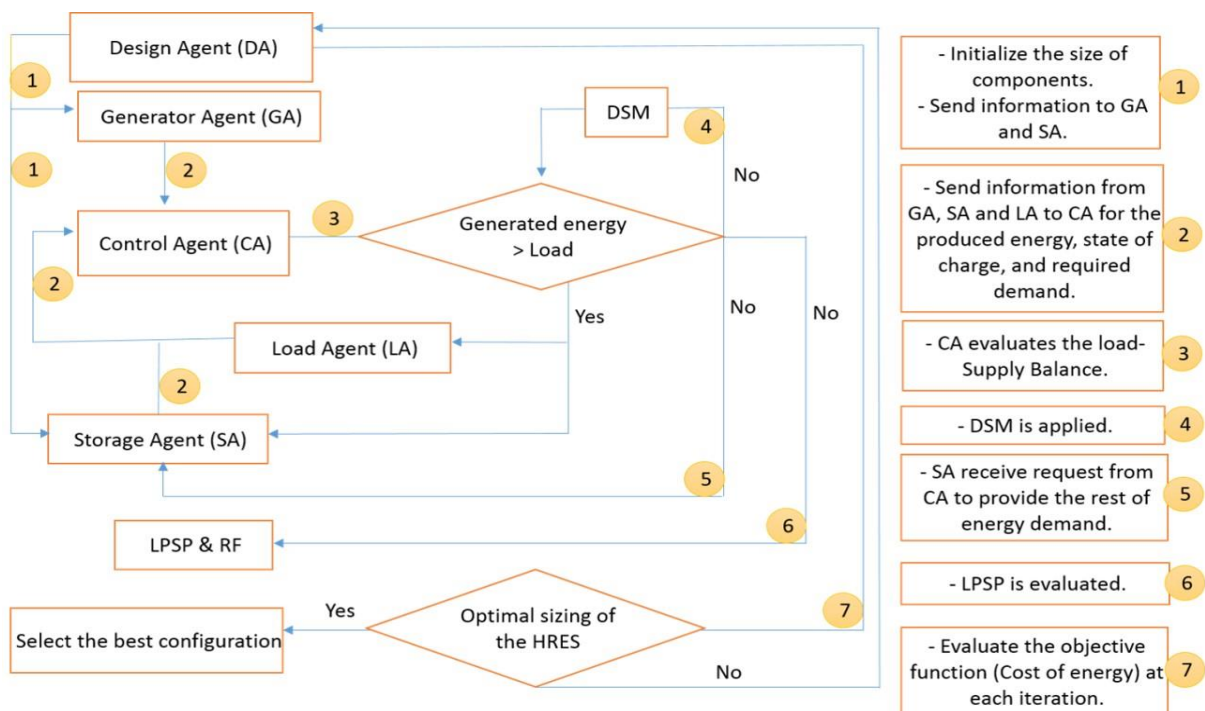


Figure 10. Flowchart of the proposed optimization model.

3. Simulation using in-house code

In this study, a MATLAB code has been developed and implemented to optimize the proposed HRES. First, the modelling of five agents is performed. Each agent is defined as a function file. The design agent includes two sub-agents, one for implementing the particle swarm optimization algorithm, which is used to solve the multi-objective problem, and another one is created for evaluating the objective function and constraints. In the control agent, the energy management strategy is implemented including the proposed DSM strategy. In the generator agent, mathematical equations for energy sources are developed to evaluate the produced energy at each time step. The storage agent consists of two sub-agents, namely charge and discharge agents. In these two sub-agents, the state of charge of the battery bank is evaluated based on their modelling equations. The communication between these agents is defined by call functions. The required inputs data for starting the simulation are imported simultaneously to MATLAB software as vectors with a duration of 8760 hours (i.e. number of hours per year). After MATLAB completes the simulation, the results are exported for data post-processing and analysis. Finally, to validate the developed PSO-based code, HOMER Pro is used simultaneously to simulate the proposed HRES for a baseline case simulation (i.e. without DSM), as the HOMER software is unable to do the demand management.

The proposed HRES is optimized with two different scenarios according to the battery technology (L-acid and Li-ion), where a sensitivity analysis is performed by imposing different values for RF_{minimum} , ranging from 0 % to 100%. Furthermore, two simulation scenarios are investigated based on the proposed DSM strategy which are integrated with the PSO-based algorithm. The description of these two scenarios is as follows.

3.1. First scenario

In this scenario, the optimal sizing of the HRES is performed without introducing the suggested DSM strategy in the optimisation. However, a supply-side management strategy is applied in order to control the operation of the HRES. Here, the annual electricity demand of the studied building is evaluated for a desired set point temperature of 24 °C (which represents the temperature for high thermal comfort requirements in cooling mode). This scenario is also simulated by HOMER software to verify the accuracy of the developed MATLAB code.

3.2. Second scenario

In this scenario, the suggested DSM (that includes peak load shaving strategy and supply-side management) is integrated into the developed PSO-based MATLAB code, in which two different loads for the same building are imported to MATLAB software to perform the simulations. The first load incorporated the evaluated demand for cooling at 24°C (i.e. a standard desired temperature of cooling mode). The second load is obtained by increasing the energy demand for cooling in case of setting the desired temperature at 29°C. After applying the proposed DSM strategy, the operating energy demand for the building is obtained, in which at each time step (hour), the energy demand for the building takes one value from the two candidate loads (either from the first load or the second load) depending on the available energy produced from renewable sources. When the energy generated from renewable sources is greater than the value of power from the first load, in this case, the operation demand for the building takes the value of power from the first load; otherwise, it takes the value from the second load. After finishing 8760 hours, the yearly operating load for the building is obtained, and based on this, the objective functions are evaluated.

4. Results and Discussion

The design and techno-economic evaluation of the proposed HRES are carried out using the developed optimisation approach. After that, the obtained results with the developed MATLAB code and by HOMER software are first compared for validation purposes. Then the results for all investigated scenarios are presented and discussed.

4.1. Validation of the developed model

Here, the developed MATLAB code is validated according to a baseline scenario with condition of $RF=100\%$. Fig. 11 shows the convergence of the developed PSO-based code, in case of using (a) L-acid batteries and (b) Li-ion batteries, respectively and for the two investigated scenarios (with and without applying the suggested DSM).

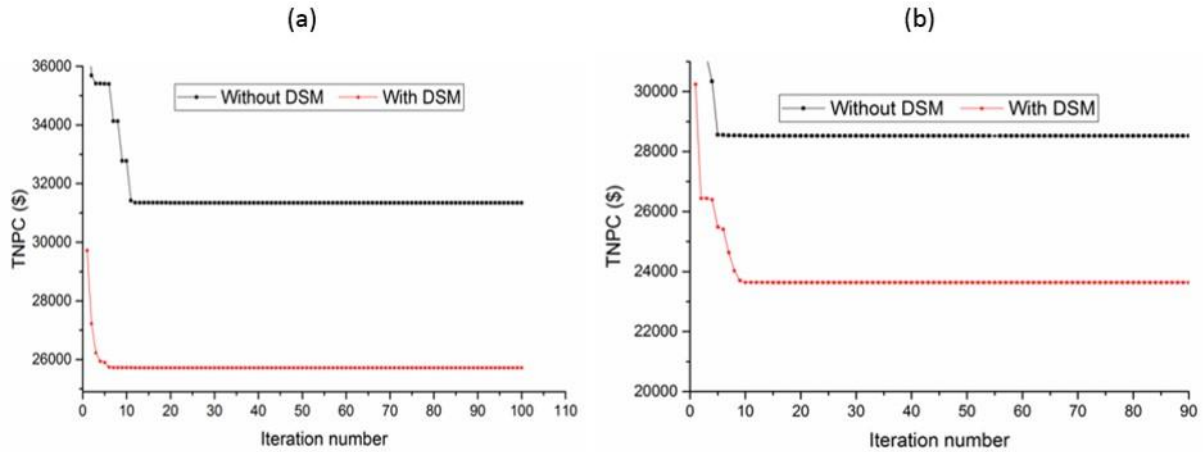


Figure 11. The convergence of PSO-based MATLAB code for HRES with (a) L-acid batteries; (b) Li-ion batteries.

The comparisons between the obtained results by the MATLAB code and HOMER software for a baseline scenario (with RF=100% and without DSM) are presented in Table 6.

Table 6. Validation of the developed optimization model with HOMER

| Optimizer | PV (kW) | WT (Nbr) | DG (kW) | L-acid (kWh) | Li-ion (kWh) | Converter (kW) | TNPC (\$) | LPSP (%) | COE (\$) | Initial cost (\$) | Excess (kWh/year) |
|-----------|---------|----------|---------|--------------|--------------|----------------|-----------|----------|----------|-------------------|-------------------|
| HOMER | 8.61 | 0 | 0 | / | 15 | 3.32 | 27361 | 2.1 | 0.25 | 20603 | 8478 |
| PSO | 8.38 | | | / | 15 | 4.45 | 28314 | 2 | 0.26 | 21018 | 6494 |
| HOMER | 8.96 | 0 | 0 | 20 | / | 3.44 | 31110 | 2.1 | 0.29 | 20337 | 8801 |
| PSO | 8.42 | | | 20 | / | 4.45 | 31379 | 2 | 0.29 | 20187 | 6569 |

It can be seen that the obtained results by the developed model are in good agreement with those obtained by HOMER software, with small and acceptable differences. Furthermore, the calculation time required for obtaining results within the developed code is lower compared to the HOMER simulation. Moreover, the implemented PSO-based code is converged rapidly, same as those in ref [53,54]. Hence, the accuracy of the implemented MATLAB code has been validated and the simulation of the HRES can be continued for the other scenarios. As mentioned, a DSM strategy is implemented and tested under a case study of a typical residential building, and the aim is to reduce the system investment cost, as well as the primary and dumped loads, simultaneously. This approach has clear benefits compared to most previous works that merely carried out the optimal sizing of HRESs by focusing on the reduction of the system cost while the satisfaction of the load demand even in case of an overload demand were likely leading to the high investment cost and the large dumped load.

4.2. HRES's design with a high renewable fraction

In the first simulation case, $RF_{\text{minimum}}=100\%$ is imposed in the optimization, in which the proposed HRES is simulated with both L-acid and Li-ion battery characteristics.

After the simulation, the results of optimal design for the HRES with L-acid batteries are given in Table 7 and Table 8, respectively.

Table 7. HRES's design within L-acid battery with RF=100%

| RF_{minimum} (%) | DSM | PV (kW) | WT (Nbr) | DG (kW) | L-acid (kWh) | Converter (kW) | TNPC (\$) | RF (%) | LPSP (%) |
|---------------------------|-----|---------|----------|---------|--------------|----------------|-----------|--------|----------|
| 100 | NO | 8.42 | 0 | 0 | 20 | 4.45 | 31379 | 100 | 2 |
| | YES | 6.96 | 0 | 0 | 16 | 4.18 | 25717 | 100 | 2 |
| Only DG | | 0 | 0 | 4 | 0 | 0 | 26664 | 0 | 0.05 |

Table 8. HRES's design within L-acid battery with RF=100% (Continue)

| RF _{minimum} (%) | DSM | COE (\$/kWh) | Fuel (L/year) | CO2 (Kg/year) | Excess (kWh) | load_24 (kWh) | Load_29 (kWh) | Demand (kWh) |
|------------------------------|-----|-----------------|------------------|------------------|-----------------|------------------|------------------|-----------------|
| 100 | NO | 0.29 | 0 | 0 | 6569 | 8698 | 6948 | 8698 |
| | YES | 0.26 | 0 | 0 | 4648 | 8698 | 6948 | 8050 |
| Only DG | | 0.245 | 4993 | 11983 | 0 | 8698 | 6948 | 8698 |

Similarly, the results of optimal design for the HRES with Li-ion battery characteristics are summarized in Table 9 and Table 10, respectively.

Table 9. HRES's design within Li-ion battery with RF=100%

| RF _{minimum} (%) | DSM | PV (kW) | WT (Nbr) | DG (kW) | Li-ion (kWh) | Converter (kW) | TNPC (\$) | RF (%) | LPSP (%) |
|------------------------------|-----|------------|-------------|------------|-----------------|-------------------|--------------|-----------|-------------|
| 100 | NO | 8.38 | 0 | 0 | 15 | 4.45 | 28314 | 100 | 2 |
| | YES | 7 | 0 | 0 | 11 | 4.18 | 23427 | 100 | 2 |
| 0 | NO | 0.68 | 0 | 3 | 0 | 0.59 | 19422 | 15 | 1.39 |
| | YES | 0.21 | 1 | 2 | 0 | 2.17 | 18383 | 66 | 1.43 |
| Only DG | | 0 | 0 | 4 | 0 | 0 | 26664 | 0 | 0.05 |

Table 10. HRES's design within Li-ion battery with RF=100% (Continue)

| RF _{minimum} (%) | DSM | COE (\$/kWh) | Fuel (L/year) | CO2 (Kg/year) | Excess (kWh) | load_24 (kWh) | Load_29 (kWh) | Demand (kWh) |
|------------------------------|-----|-----------------|------------------|------------------|-----------------|------------------|------------------|-----------------|
| 100 | NO | 0.26 | 0 | 0 | 6494 | 8698 | 6948 | 8698 |
| | YES | 0.23 | 0 | 0 | 4725 | 8698 | 6948 | 8055 |
| 0 | NO | 0.18 | 3904 | 9370 | 7 | 8698 | 6948 | 8698 |
| | YES | 0.21 | 1667 | 4001 | 2598 | 8698 | 6948 | 7052 |
| Only DG | | 0.245 | 4993 | 11983 | 0 | 8698 | 8698 | 6948 |

Furthermore, the contributions of the HRES's components in case of using L-acid and Li-ion batteries are presented in Fig. 12 and Fig. 13, respectively.

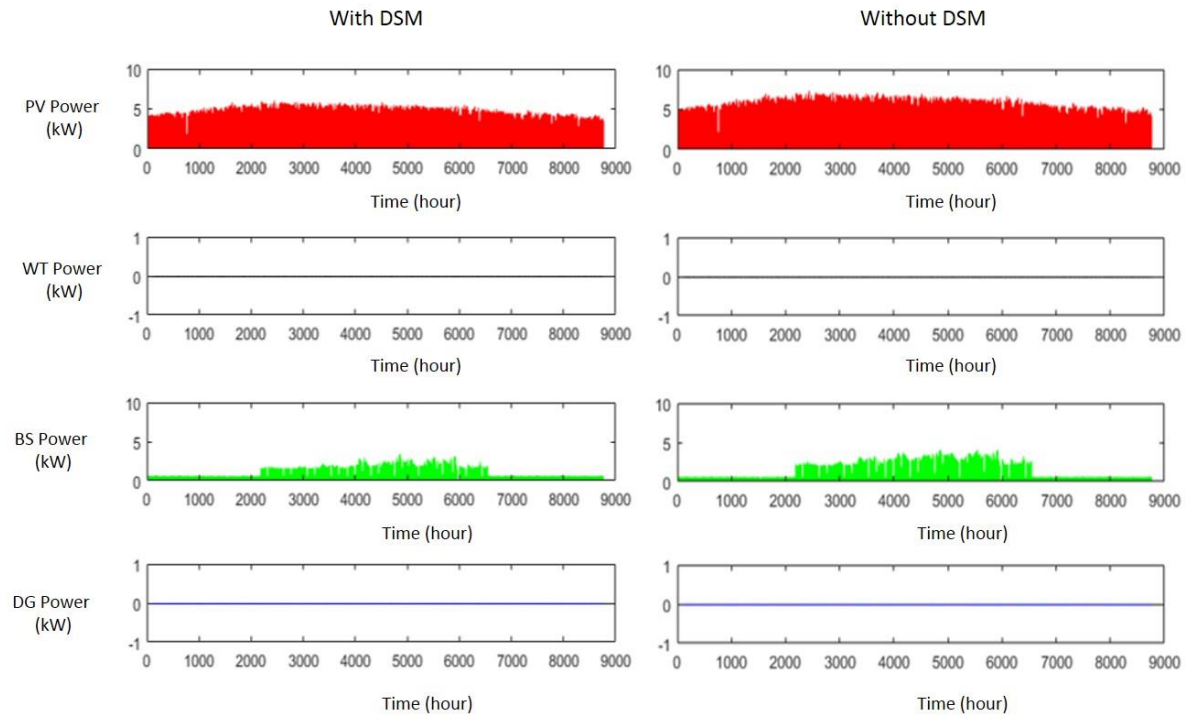


Figure 12. Contribution of HRES's components for HRES with L-acid batteries (RF=100%).

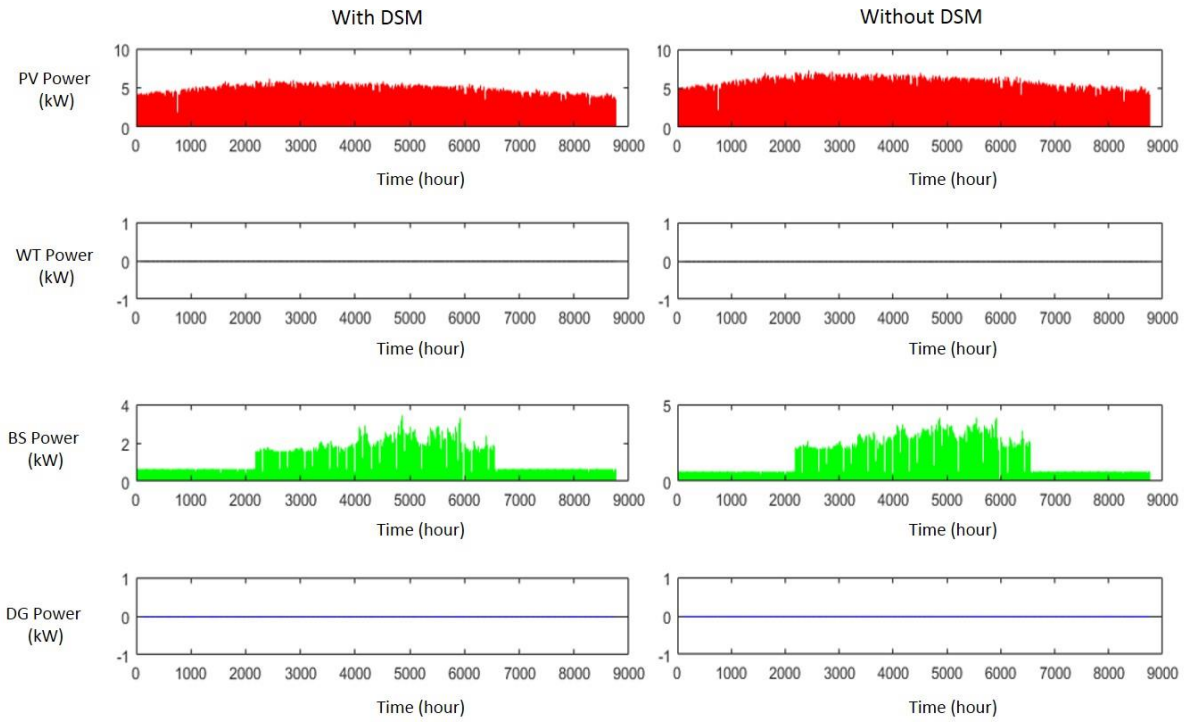


Figure 13. Contribution of HRES's components for HRES with Li-ion batteries (RF=100%).

The hourly energy demand of the building for both scenarios using L-acid and Li-ion batteries are presented in Fig. 14 and Fig. 15, respectively.

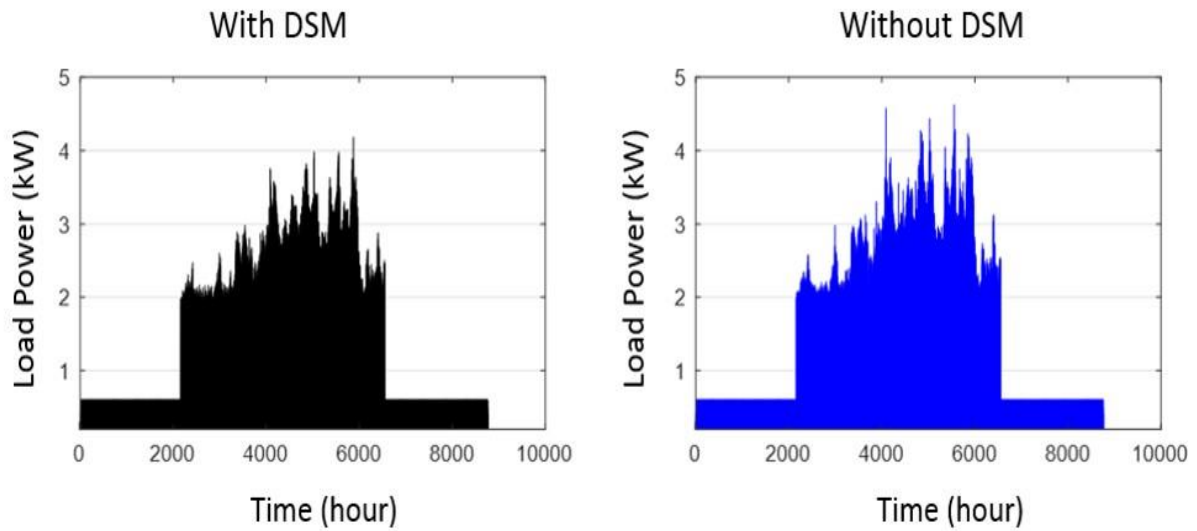


Figure 14. Load power for HRES with L-acid batteries (RF=100%).

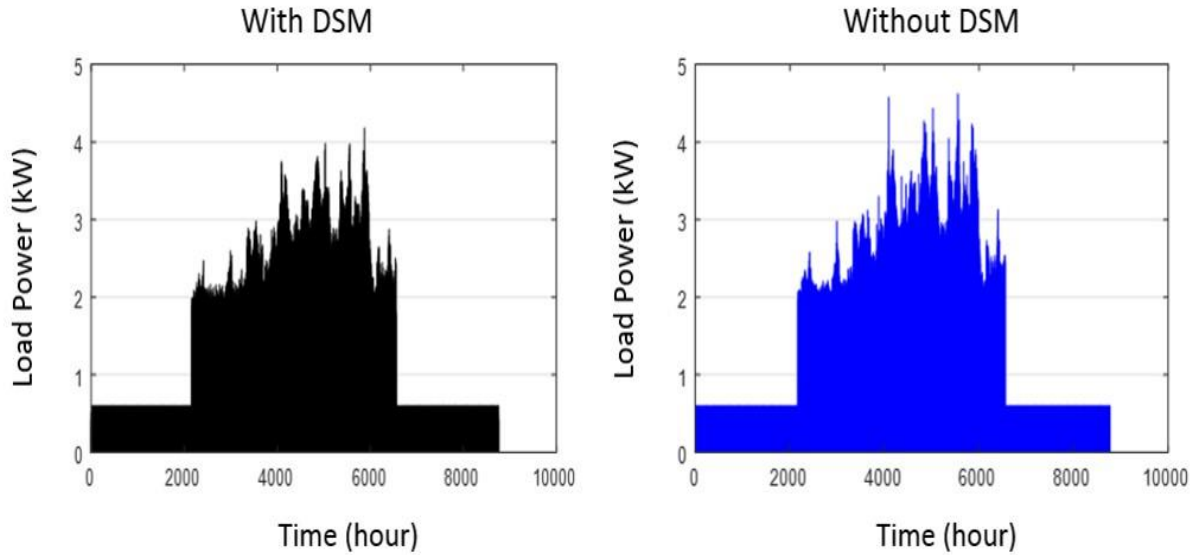


Figure 15. Load power for HRES with Li-ion batteries (RF=100%).

From the obtained results and as shown in Figs. 14, 15, for high RF values (100%), the energy demand for the building can be reduced by 7% for both cases (i.e. using L-acid or Li-ion batteries) while applying the suggested DSM. Moreover, the amount of electricity excess or dumped load is also reduced compared to the case without DSM. Reducing the dumped load is an important factor, as the investment cost of renewable-based HRESs is still very high for customers in the developing countries. Besides that, for both investigated scenarios and using both battery technologies, the obtained optimal HRES configurations consist of PV and battery storage. However, applying the DSM, the capacity of battery storage can be largely reduced by 25% and the capacity of PV modules can be slightly reduced, which leads to an overall 18% reduction on both TNPC. Of this, the HRES that includes PV and L-acid has a COE of 0.29\$/kWh (without DSM) and 0.26\$/kWh (with DSM) which makes this configuration only attractive when considering renewability preferences. However, for PV/battery (Li-ion), the COE can be reduced from 0.26 \$/kWh (without DSM) to 0.23 \$/kWh (with DSM), which makes this configuration more cost-effective than using a stand-alone DG system. Moreover, this configuration is more interesting than using solely DG, considering the effect on the environment and the local government policy that encourages solutions for saving fossil fuels. Hence, it can be concluded that within high renewable contribution (RF=100%), PV/battery (Li-ion) using the suggested DSM technique is the optimum solution for the electrification of the studied building.

4.3. HRES's design with a low renewable fraction

In this case, the minimum RF value is imposed at 0% for the optimization. Table 11 and Table 12 provide the results for this simulation case, using the characteristics of both battery technologies (i.e. L-acid or L-ion).

Table 11. HRES's design results with RF_{minimum} = 0%

| RF _{minimum} (%) | DSM | PV (kW) | WT (Nbr) | DG (kW) | BS (kWh) | Converter (kW) | TNPC (\$) | RF (%) | LPSP (%) |
|---------------------------|-----|---------|----------|---------|----------|----------------|-----------|--------|----------|
| 0 | NO | 0.68 | 0 | 3 | 0 | 0.59 | 19422 | 15 | 1.39 |
| | YES | 0 | 1 | 2 | 0 | 2.17 | 18471 | 63 | 1.53 |
| Only DG | | 0 | 0 | 4 | 0 | 0 | 26664 | 0 | 0.05 |

Table 12. HRES's design results with RF_{minimum} = 0% (Continue)

| RF _{minimum} (%) | DSM | COE (\$/kWh) | Fuel (L/year) | CO2 (Kg/year) | Excess (kWh) | load_24 (kWh) | Load_29 (kWh) | Demand (kWh) |
|---------------------------|-----|--------------|---------------|---------------|--------------|---------------|---------------|--------------|
| 0 | NO | 0.18 | 3904 | 9370 | 7 | 8698 | 6948 | 8698 |
| | YES | 0.21 | 1757 | 4217 | 2135 | 8698 | 6948 | 7028 |
| Only DG | | 0.245 | 4993 | 11983 | 0 | 8698 | 8698 | 6948 |

With $RF_{\text{minimum}} = 0\%$, the contribution of the HRES's components and the hourly energy demand of the building is presented in Fig. 16 and Fig. 17, respectively.

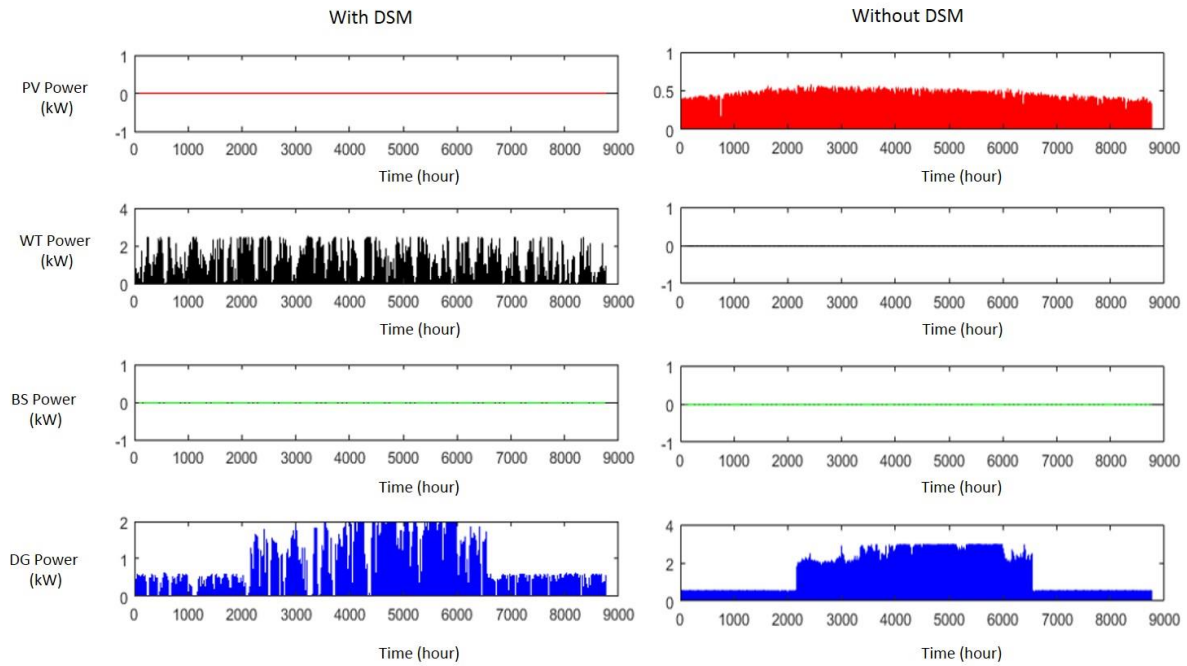


Figure 16. Contribution of HRES's components for HRES with $RF_{\text{minimum}} = 0\%$.

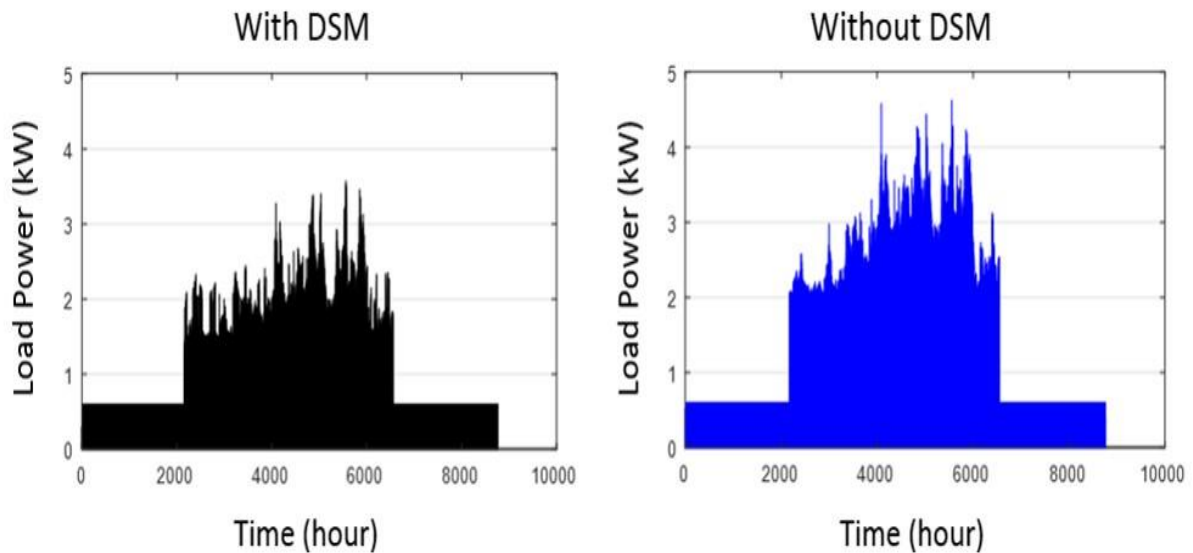


Figure 17. Energy demand for HRES with $RF_{\text{minimum}} = 0\%$.

By imposing a minimum $RF = 0\%$ and without applying the proposed DSM technique, PV/diesel is found to be the best configuration. In this case, a low renewable fraction is reached (15%), in which the majority of load demand is supplied by DG and with slight contribution from PV modules. However, after introducing the DSM strategy in the optimization, the optimal HRES configuration includes a small wind turbine and DG. In this case, the building energy consumption is decreased by 19% and the contribution of DG is reduced extensively, where a RF equal to 63% and a COE of 0.21 \$/kWh are reached. However, for both scenarios (with and without DSM), it can be seen that no battery storage is required as the wind turbine can work in the daytime as well as in the night time. It is concluded that with low RF values, the COE for both scenarios is lower than in the case of using a stand-alone DG system. Nevertheless, while applying the DSM, the renewable energy contribution is increased

noticeably. Therefore, wind/DG HRES is the best configuration for the case study building with low renewable fraction values.

4.4. Comparing results and summary

The results indicate that the TNPC and COE of the HRES can be increased while increasing the contribution of renewable energy. Conversely, CO₂ emission and fuel consumption can also be reduced. Hence, the design of the best HRES that presents optimality from techno-economic and environment perspectives is one of the main reasons for performing sensitivity analysis on renewable fraction and component characteristics.

With RF_{minimum} = 0%, it is found that the COE of the obtained HRES is smaller than the value of the COE obtained with using a stand-alone DG system that is merely 0.245\$/kWh.

Comparing the obtained results, the following improvements can be made by introducing the suggested DSM: i.e. with RF = 100%, the energy demand, TNPC and electricity excess are decreased by 7%, 18% and 29%, respectively. In such a case, the best solution includes PV/battery (Li-ion), with the TNPC and COE being 23,427\$ and 0.23\$/kWh, respectively. However, by imposing 0 % as minimum RF, the energy demand is reduced by 19% and fuel consumption and CO₂ emissions are minimized by 57%. Conversely, the RF is raised from 15% (using solely Supply-side management) to 63% (DSM) where the optimal configuration consists of PV/wind/diesel, with COE of 0.21\$/kWh, which is smaller than that using a stand-alone DG. Moreover, for both simulation cases, small-scale WTs do not provide viable solution without applying the proposed DSM strategy, despite that the present case study has already considered the windiest location in the country. These results have demonstrated that the investment cost of small-scale WT is still very high compared to PV modules.

The findings of this work have proved the effectiveness of the suggested approach, as it is able to address the demand-supply mismatch problem, limit the oversizing of components and reduce the building energy demand. Further extending this model to include additional influencing criteria, such as thermal comfort requirements and occupant preferences would broaden the optimization potential of the proposed method. We anticipate additional changes to be made, however these are outside the scope of this paper and are subjects for future studies. (in my view this part should be in the conclusion and further work section).

5. Conclusions and Further work

This paper has presented a novel approach for managing both the demand and supply sides through integrating a demand-supply management technique with a PSO-based algorithm for reducing building energy consumption and thus meeting the load demand at the lowest possible costs. The novelty of this work is related to the integrated demand-supply management strategy, which is based on the state of supply system and the operation of the air conditioner, i.e. we have developed a control system in which the set point temperature for air conditioner is changed (between 24 °C and 29°C according to the available energy from renewable sources).

From the obtained results, the following improvements are achieved by integrating the proposed DSM. First, with high renewable contribution, the energy demand and TNPC are decreased by 7% and 18%, respectively, for which, PV/battery (Li-ion) is found to be the best configuration, with TNPC and COE of 23,427\$ and 0.23\$/kWh, respectively. Second, with low renewable usage, the following reductions are observed including the building energy demand (19%) and both fuel consumption and CO₂ emissions (57%). In contrast, the RF is raised from 15% (without DSM) to 63% (with DSM), where the optimal configuration consists of wind/diesel, with COE 0.21\$/kWh, being smaller than that using a stand-alone DG.

The findings of this work have proved the effectiveness of the suggested approach for the chosen case study in terms of location and layout. Future work can be followed, e.g. for creating a generalized model feasible for other locations and layouts in the country and beyond. In addition, the practical implementation of the proposed design will be explored using, for instance, a combination of JADE software, Arduinos and Simulink. The thermal comfort level should also be investigated by exploring the effects of a wider range of set temperatures for cooling.

Acknowledgment

The first author would like to thank the research team of VPRS laboratory and the University of Kasdi Merbah Ouargla for their support. Many thanks also go to DGRSDT of the Ministry for Scientific Research, Algeria. He also wishes to thank the Engineering Modelling and Simulation research group at the Department of Engineering,

Design and Mathematics, University of the West of England, Bristol, UK for hosting his short study abroad during a research visit.

References

- [1] Ahmad MW, Mourshed M, Yuce B, Rezgui Y. Computational intelligence techniques for HVAC systems : A review. *Build Simul* 2016;359–98. doi:10.1007/s12273-016-0285-4.
- [2] Mokhtara C., Negrou B., Settou N., Gouareh A., Settou B. CMA. Decision-making and optimal design of off-grid hybrid renewable energy system for electrification of mobile buildings in Algeria: case study of drilling camps in Adrar. *Alger J Env Sc Technol* 2020.
- [3] L'Energie M de. Bilan des réalisations du secteur de l'Energie 2018. doi:http://www.energy.gov.dz/francais/uploads/MAJ_2018/Stat/Bilan_des_Realisations_du_secteur_2017_%C3%A9dition_2018.pdf.
- [4] Government A. Renewable Energy and Energy Efficiency Development Plan 2015-2030. IEA 2015. <https://www.iea.org/policiesandmeasures/renewableenergy/?country=ALGERIA>.
- [5] Haddoum S, Bennour H, Zaïd TA. Algerian Energy Policy : Perspectives , Barriers , and Missed Opportunities. vol. 1700134. 2018. doi:10.1002/gch2.201700134.
- [6] Thiaux Y, Dang TT, Schmerber L, Multon B, Ben Ahmed H, Bacha S, et al. Demand-side management strategy in stand-alone hybrid photovoltaic systems with real-time simulation of stochastic electricity consumption behavior. *Appl Energy* 2019;253:113530. doi:10.1016/j.apenergy.2019.113530.
- [7] Hossain MA, Pota HR, Squartini S, Zaman F, Guerrero JM. Energy scheduling of community microgrid with battery cost using particle swarm optimisation. *Appl Energy* 2019;254:113723. doi:10.1016/j.apenergy.2019.113723.
- [8] Faccio M, Gamberi M, Bortolini M, Nedaei M. State-of-art review of the optimization methods to design the configuration of hybrid renewable energy systems (HRESs). *Front Energy* 2018;12:591–622. doi:10.1007/s11708-018-0567-x.
- [9] Mehrjerdi H. Modeling, integration, and optimal selection of the turbine technology in the hybrid wind-photovoltaic renewable energy system design. *ENERGY Convers Manag* 2020;205:112350. doi:10.1016/j.enconman.2019.112350.
- [10] Abo-elyousr FK, Nozhy AN. Bi-objective Economic Feasibility of Hybrid Micro- Grid Systems with Multiple Fuel Options for Islanded Areas in Egypt. *Renew Energy* 2018. doi:10.1016/j.renene.2018.05.066.
- [11] Ma T, Javed MS. Integrated sizing of hybrid PV-wind-battery system for remote island considering the saturation of each renewable energy resource. *ENERGY Convers Manag* 2019;182:178–90. doi:10.1016/j.enconman.2018.12.059.
- [12] Assaf J, Shabani B. A novel hybrid renewable solar energy solution for continuous heat and power supply to standalone-alone applications with ultimate reliability and cost effectiveness. *Renew Energy* 2019;138:509–20. doi:10.1016/j.renene.2019.01.099.
- [13] Tudu B, Mandal KK, Chakraborty N. Optimal design and development of PV-wind-battery based nano-grid system: A field-on-laboratory demonstration. *Front Energy* 2019;13:269–83. doi:10.1007/s11708-018-0573-z.
- [14] Dufo-López R, Champier D, Gibout S, Lujano-Rojas JM, Domínguez-Navarro JA. Optimisation of off-grid hybrid renewable systems with thermoelectric generator. *ENERGY Convers Manag* 2019;196:1051–67. doi:10.1016/j.enconman.2019.06.057.
- [15] Adefarati T, Bansal RC. Reliability , economic and environmental analysis of a microgrid system in the presence of renewable energy resources. *Appl Energy* 2019;236:1089–114. doi:10.1016/j.apenergy.2018.12.050.
- [16] Jamshidi M, Askarzadeh A. Techno-economic analysis and size optimization of an off-grid hybrid photovoltaic , fuel cell and diesel generator system. *Sustain Cities Soc* 2019;44:310–20. doi:10.1016/j.scs.2018.10.021.
- [17] Moradi H, Esfahanian M, Abtahi A, Zilouchian A. Optimization and energy management of a standalone hybrid microgrid in the presence of battery storage system. *Energy* 2018. doi:10.1016/j.energy.2018.01.016.
- [18] Eriksson EL V, Gray EM. Optimization of renewable hybrid energy systems – A multi-objective approach. *Renew Energy* 2018. doi:10.1016/j.renene.2018.10.053.
- [19] Zhang W, Maleki A, Rosen MA, Liu J. Optimization with a simulated annealing algorithm of a hybrid system for renewable energy including battery and hydrogen storage. *Energy* 2018;163:191–207. doi:10.1016/j.energy.2018.08.112.
- [20] Zhang W, Maleki A, Rosen MA, Liu J. Sizing a stand-alone solar-wind-hydrogen energy system using weather forecasting and a hybrid search optimization algorithm. *ENERGY Convers Manag* 2019;180:609–21. doi:10.1016/j.enconman.2018.08.102.

- [21] Mellouk L, Ghazi M, Aaroud A, Boulmalf M, Benhaddou D, Zine-dine K. Design and energy management optimization for hybrid renewable energy system- case study : Laayoune region. *Renew Energy* 2019;139:621–34. doi:10.1016/j.renene.2019.02.066.
- [22] Yu H, Zhang C, Deng Z, Bian H, Sun C, Jia C. Economic optimization for configuration and sizing of micro integrated energy systems. *J Mod Power Syst Clean Energy* 2018;6:330–41. doi:10.1007/s40565-017-0291-2.
- [23] Kaabeche A, Bakelli Y. Renewable hybrid system size optimization considering various electrochemical energy storage technologies. *ENERGY Convers Manag* 2019;193:162–75. doi:10.1016/j.enconman.2019.04.064.
- [24] Hamanah WM, Abido MA, Alhems LM. Optimum Sizing of Hybrid PV, Wind, Battery and Diesel System Using Lightning Search Algorithm. *Arab J Sci Eng* 2019. doi:10.1007/s13369-019-04292-w.
- [25] Haratian M, Tabibi P, Sadeghi M, Vaseghi B, Poustdouz A. A renewable energy solution for stand-alone power generation: A case study of KhshU Site-Iran. *Renew Energy* 2018;125:926–35. doi:10.1016/j.renene.2018.02.078.
- [26] Fodhil F, Hamidat A, Nadjemi O. Energy Control Strategy Analysis of Hybrid Power Generation System for Rural Saharan Community in Algeria. *Lect Notes Networks Syst* 2018;35:108–20. doi:10.1007/978-3-319-73192-6_12.
- [27] Fodhil F, Hamidat A, Nadjemi O. Potential , optimization and sensitivity analysis of photovoltaic-diesel-battery hybrid energy system for rural electricity in Algeria. *Energy* 2019;169:613–24. doi:10.1016/j.energy.2018.12.049.
- [28] Duman AC, Güler Ö. Techno-economic analysis of off-grid PV / wind / fuel cell hybrid system combinations with a comparison of regularly and seasonally occupied households. *Sustain Cities Soc* 2018;42:107–26. doi:10.1016/j.scs.2018.06.029.
- [29] Anoune K, Laknizi A, Bouya M, Astito A, Ben Abdellah A. Sizing a PV-Wind based hybrid system using deterministic approach. *ENERGY Convers Manag* 2018;169:137–48. doi:10.1016/j.enconman.2018.05.034.
- [30] Jafar M, Moghaddam H, Kalam A, Arabi S. Optimal sizing and energy management of stand-alone hybrid photovoltaic / wind system based on hydrogen storage considering LOEE and LOLE reliability indices using flower pollination algorithm. *Renew Energy* 2019;135:1412–34. doi:10.1016/j.renene.2018.09.078.
- [31] Das M, Anil M, Singh K, Biswas A. Techno-economic optimization of an off-grid hybrid renewable energy system using metaheuristic optimization approaches – Case of a radio transmitter station in India. *ENERGY Convers Manag* 2019;185:339–52. doi:10.1016/j.enconman.2019.01.107.
- [32] Halabi LM, Mekhilef S, Olatomiwa L, Hazelton J. Performance analysis of hybrid PV/diesel/battery system using HOMER: A case study Sabah, Malaysia. *ENERGY Convers Manag* 2017;144:322–39. doi:10.1016/j.enconman.2017.04.070.
- [33] Rullo P, Braccia L, Luppi P, Zumoffen D, Feroldi D. Integration of sizing and energy management based on economic predictive control for standalone hybrid renewable energy systems. *Renew Energy* 2019;140:436–51. doi:10.1016/j.renene.2019.03.074.
- [34] Anvari-moghaddam A, Rahimi-kian A, Mirian MS, Guerrero JM. A multi-agent based energy management solution for integrated buildings and microgrid system. *Appl Energy* 2017;203:41–56. doi:10.1016/j.apenergy.2017.06.007.
- [35] Uddin M, Romlie MF, Abdullah MF, Abd Halim S, Abu Bakar AH, Chia Kwang T. A review on peak load shaving strategies. *Renew Sustain Energy Rev* 2018;82:3323–32. doi:10.1016/j.rser.2017.10.056.
- [36] Tu T, Rajarathnam GP, Vassallo AM. Optimization of a stand-alone photovoltaic e wind e diesel e battery system with multi-layered demand scheduling. *Renew Energy* 2019;131:333–47. doi:10.1016/j.renene.2018.07.029.
- [37] Zheng Y, Jenkins BM, Kornbluth K, Kendall A, Træholt C. Optimization of a biomass-integrated renewable energy microgrid with demand side management under uncertainty. *Appl Energy* 2018;230:836–44. doi:10.1016/j.apenergy.2018.09.015.
- [38] Yang F, Xia X. Techno-economic and environmental optimization of a household photovoltaic-battery hybrid power system within demand side management. *Renew Energy* 2017. doi:10.1016/j.renene.2017.02.054.
- [39] Sarkar T, Bhattacharjee A, Samanta H, Bhattacharya K, Saha H. Optimal design and implementation of solar PV-wind-biogas-VRFB storage integrated smart hybrid microgrid for ensuring zero loss of power supply probability. *ENERGY Convers Manag* 2019;191:102–18. doi:10.1016/j.enconman.2019.04.025.
- [40] Wu Z, Tazvinga H, Xia X. Demand side management of photovoltaic-battery hybrid system. *Appl Energy* 2015;148:294–304. doi:10.1016/j.apenergy.2015.03.109.
- [41] Mohseni S, Brent AC, Burmester D. A demand response-centred approach to the long-term equipment capacity planning of grid-independent micro-grids optimized by the moth-flame optimization algorithm.

- ENERGY Convers Manag 2019;200:112105. doi:10.1016/j.enconman.2019.112105.
- [42] Mokhtara C, Negrou B, Settou N, Gouareh, Abderrahmane BS. Pathways to plus-energy buildings in Algeria : design optimization method based on GIS and multi-criteria decision-making. *Energy Procedia* 2019;162:171–80. doi:10.1016/j.egypro.2019.04.019.
- [43] EnergyPlus n.d. <https://energyplus.net> (accessed June 11, 2020).
- [44] El-bidairi KS, Duc H, Jayasinghe SDG, Mahmoud TS, Penesis I. A hybrid energy management and battery size optimization for standalone microgrids : A case study for Flinders Island , Australia. *ENERGY Convers Manag* 2018;175:192–212. doi:10.1016/j.enconman.2018.08.076.
- [45] Mandal S, Das BK, Hoque N. Optimum sizing of a stand-alone hybrid energy system for rural electrification in Bangladesh. *J Clean Prod* 2018;200:12–27. doi:10.1016/j.jclepro.2018.07.257.
- [46] Mohamed MA, Eltamaly AM, Alolah AI, Hatata AY, Mohamed MA, Eltamaly AM, et al. A novel framework-based cuckoo search algorithm for sizing and optimization of grid-independent hybrid renewable energy systems. *Int J Green Energy* 2018;00:1–15. doi:10.1080/15435075.2018.1533837.
- [47] Mousavi N, Kothapalli G, Habibi D, Das CK, Baniyasi A. A novel photovoltaic-pumped hydro storage microgrid applicable to rural areas. *Appl Energy* 2020;262:114284. doi:10.1016/j.apenergy.2019.114284.
- [48] Das BK, Zaman F. Performance analysis of a PV/Diesel hybrid system for a remote area in Bangladesh: Effects of dispatch strategies, batteries, and generator selection. *Energy* 2019;169:263–76. doi:10.1016/j.energy.2018.12.014.
- [49] Pro H. Renewable fraction n.d. https://www.homerenergy.com/products/pro/docs/latest/_renewable_fraction.html (accessed June 12, 2020).
- [50] Shara M, Elmekawy TY. Multi-objective optimal design of hybrid renewable energy systems using PSO-simulation based approach. *Renew Energy* 2014;68. doi:10.1016/j.renene.2014.01.011.
- [51] Twaha S, Ramli MAM. A review of optimization approaches for hybrid distributed energy generation systems: Off-grid and grid-connected systems. *Sustain Cities Soc* 2018;41:320–31. doi:10.1016/j.scs.2018.05.027.
- [52] Mohamed MA, Eltamaly AM, Alolah AI. Sizing and techno-economic analysis of stand-alone hybrid photovoltaic / wind / diesel / battery power generation systems 2015. doi:10.1063/1.4938154.
- [53] Samy MM, Barakat S, Ramadan HS. A flower pollination optimization algorithm for an off-grid PV-Fuel cell hybrid renewable system. *Int J Hydrogen Energy* 2019;44:2141–52. doi:10.1016/j.ijhydene.2018.05.127.
- [54] Samy MM, Barakat S, Ramadan HS. Techno-economic analysis for rustic electrification in Egypt using multi-source renewable energy based on PV/ wind/ FC. *Int J Hydrogen Energy* 2019. doi:10.1016/j.ijhydene.2019.04.038.